



## An analytical solution and case study of groundwater head response to dual tide in an island leaky confined aquifer

Pingping Sun,<sup>1</sup> Hailong Li,<sup>1,2</sup> Michel C. Boufadel,<sup>3</sup> Xiaolong Geng,<sup>2,4</sup> and Shi Chen<sup>1</sup>

Received 1 February 2008; revised 26 August 2008; accepted 4 September 2008; published 9 December 2008.

[1] This paper presents an analytical solution of groundwater head response to dual-tide fluctuation in the transect of an island leaky aquifer system comprising a confined aquifer and its overlying semipermeable confining layer. Both layers terminate at the coastlines on two sides of the island. Solution analysis indicates that the tidal waves from the two sides of the island transect interfere at the middle of the island and the interference decreases to zero as the horizontal length of the aquifer increases to infinity. The leakage of the overlying confining layer enhances the landward attenuation of the tidal head fluctuation and shortens the time lag between the head and tide fluctuations. The solution agreed well with the observations in eight piezometers in Garden Island on the continental shelf of Western Australia reported by Trefry and Bekele (2004).

**Citation:** Sun, P., H. Li, M. C. Boufadel, X. Geng, and S. Chen (2008), An analytical solution and case study of groundwater head response to dual tide in an island leaky confined aquifer, *Water Resour. Res.*, 44, W12501, doi:10.1029/2008WR006893.

### 1. Introduction

[2] Ocean tides are a natural high-frequency forcing which makes the groundwater head in coastal aquifers fluctuate periodically. Analytical and numerical studies of this natural phenomenon have been conducted by many hydrologists since the 1950s. They can be divided into two classes based on aquifer complexity: single aquifer [e.g., Jacob, 1950; Drogue *et al.*, 1984; Sun, 1997; Townley, 1995; Li and Yang, 2000; Li *et al.*, 2002] and multilayered or composite aquifer system [e.g., Jiao and Tang, 1999; Trefry, 1999; Li *et al.*, 2001; Jeng *et al.*, 2002; Li and Jiao, 2001a, 2001b, 2002a, 2002b, 2003]. However, these studies are all subjected to a single tide. Rotzoll *et al.* [2008] give an analytical solution for the head distribution in a single homogeneous one-dimensional island aquifer subjected to dual tide with application in the island of Maui, Hawaii. Our paper considers a composite island aquifer system that experiences periodic forcing from opposing coastal boundaries, which can lead to integrated effects of the multitidal signals. Trefry and Bekele [2004] investigated the tide-induced groundwater level fluctuations in Garden Island, Australia. They observed and analyzed 57-day water level time series collected in 8 monitoring wells in the island. The data were used to test the utility of various simple analytical solutions of ocean tidal propagation in bounded

one-dimensional aquifers. However, all the analytical solutions that they used could not predict the observed tidal propagation bias, i.e., the inconsistency between the observed strong attenuation and small time lag. Both their numerical results and the geologic cross section information of Garden Island supported a conceptual stratigraphic model of a highly permeable, sloping stratum underlying a less permeable, superficial sand layer. On the basis of the numerical experiments, they suggested that the most probable cause of the tidal wave propagation bias was the horizontal layering in aquifer properties, and that the analysis of measured propagation bias has the potential to yield extra information on aquifer properties in the vertical direction.

[3] This paper considers an island aquifer system comprising a confined aquifer and a semipermeable layer (the confined aquifer's roof). All the layers terminate at the coastlines. The elastic storage of the aquifer's roof is neglected. The analytical solution is derived and compared with existing analytical solutions. The influence of the vertical leakage of the aquifer's semipermeable roof on the tidal groundwater flow is discussed. The new analytical solution is used to analyze the observed tidal amplitudes and time lags reported by Trefry and Bekele [2004].

### 2. Mathematical Model and Analytical Solution

#### 2.1. Mathematical Model

[4] We consider the transect of an island aquifer system comprising a confined aquifer and an overlying semipermeable layer as shown in Figure 1. We assume that the confined aquifer is horizontal, homogeneous and of uniform thickness with a length of  $L$ , and that both layers terminate at the coastlines. Following Hantush [1960] and Neuman and Witherspoon [1969], it is assumed that the flow is essentially horizontal in the confined aquifer and vertical in the semipermeable layer. Following Jiao and Tang [1999],

<sup>1</sup>School of Environmental Studies and MOE Biogeology and Environmental Geology Laboratory, China University of Geosciences, Wuhan, China.

<sup>2</sup>Department of Mathematics, Anshan Normal University, Anshan, China.

<sup>3</sup>Department of Civil and Environmental Engineering, Temple University, Philadelphia, Pennsylvania, USA.

<sup>4</sup>Department of Mathematics, Liaoning Normal University, Dalian, China.

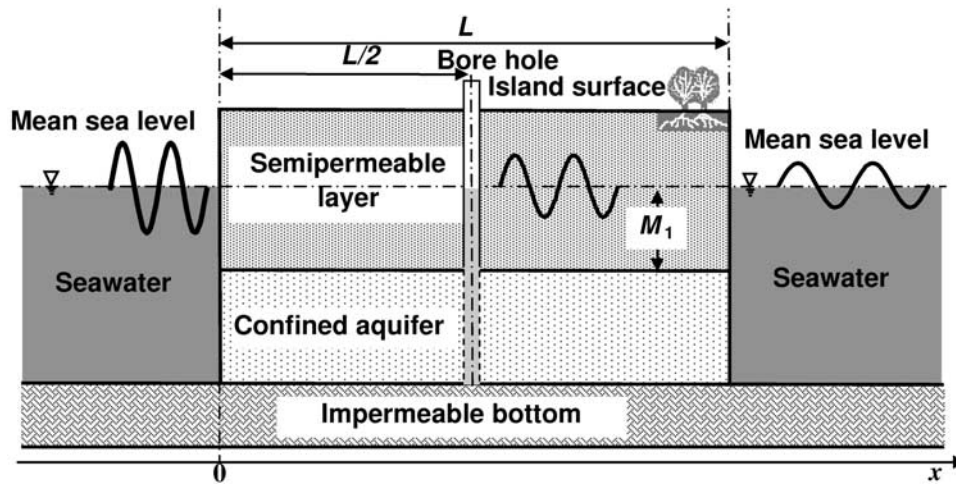


Figure 1. Schematic of the cross section of an island aquifer system subject to dual tide.

the elastic storage of the semipermeable layer and the density difference between the groundwater and the seawater are also neglected. Because the semipermeable layer is much less permeable than the aquifer, and its effective porosity is much greater than the storativity of the confined aquifer, it is reasonable to assume that the tidal fluctuation in the semipermeable layer is negligible. Here the tidal overheight is also neglected such that the water table of the semipermeable layer is a constant equal to the mean sea level.

[5] Let the  $x$  axis be perpendicular to the coastlines, horizontal, and the intersection with the left-hand side coastline be the origin of the axis (see Figure 1). The mean sea level is set to be the datum of the aquifer system. On the basis of above assumptions and the theory by Hantush [1960], the following governing equation can be used to describe the head fluctuation within the confined aquifer:

$$S \frac{\partial h}{\partial t} = T \frac{\partial^2 h}{\partial x^2} - \frac{K'}{M_1} h, 0 \leq x \leq L, \quad (1)$$

where  $t$  is the time [T],  $S$  and  $T$  are the storativity (dimensionless) and transmissivity [ $L^2 T^{-1}$ ] of the confined aquifer, respectively,  $h$  is the hydraulic head [L] of the confined aquifer,  $K'$  is the roof's vertical hydraulic conductivity [ $L T^{-1}$ ], and  $M_1$  is the average thickness (vertical distance from the mean sea level to the bottom of the semipermeable layer).

[6] Because of the linearity of the model, only one tidal constituent is considered. At the coastlines  $x = 0$  and  $x = L$ , the following Dirichlet boundary conditions are used for the dual-tide aquifer system:

$$h(x, t)|_{x=0} = A_1 \cos(\omega t) \quad (2)$$

$$h(x, t)|_{x=L} = A_2 \cos(\omega t + \theta), \quad (3)$$

where  $A_1$  and  $A_2$  denote the amplitude [L] of the tidal fluctuation on the left- and right-hand side coastal boundaries, respectively,  $\omega = 2\pi/t_0$  is the tidal frequency

[ $T^{-1}$ ] with  $t_0$  being the tidal period [T],  $\theta$  is the phase difference (radian) between the tides at both sides of the island. Note, however, according to Rotzoll *et al.* [2008] the tidal amplitude and phase may vary significantly across the island. Because of the periodicity of the solution, no initial condition is needed.

## 2.2. Analytical Solution

[7] For the sake of convenience, the following two parameters are introduced:

$$a = \sqrt{\omega S / 2T} = \sqrt{\pi S / T t_0} \quad (4)$$

$$u = \frac{K'}{M_1 \omega S}. \quad (5)$$

Here,  $a$  is the confined aquifer's tidal wave propagation parameter [ $L^{-1}$ ],  $u$  is the dimensionless leakage of the overlying semipermeable layer.

[8] Assume  $h(x, t) = \text{Re} [X(x)e^{i\omega t}]$ , where  $X(x)$  is an unknown complex function of  $x$ ,  $\text{Re}$  denotes the real part of the followed complex expression and  $i = \sqrt{-1}$ . Equations (1), (2) and (3) reduce to

$$X'' - \left( \frac{K'}{TM_1} + i\omega \frac{S}{T} \right) X = 0 \text{ with } X(x) \Big|_{x=0} = A_1$$

$$\text{and } X(x) \Big|_{x=L} = A_2 e^{i\theta}. \quad (6a)$$

Defining the eigenvalue of the differential equation in (6a) as  $\pm \lambda$  with

$$\lambda = \sqrt{\frac{K'}{TM_1} + i\omega \frac{S}{T}} = a(p + qi), \quad (6b)$$

where

$$p(u) = \sqrt{\sqrt{u^2 + 1} + u}$$

$$q(u) = \sqrt{\sqrt{u^2 + 1} - u}, \quad (6c)$$

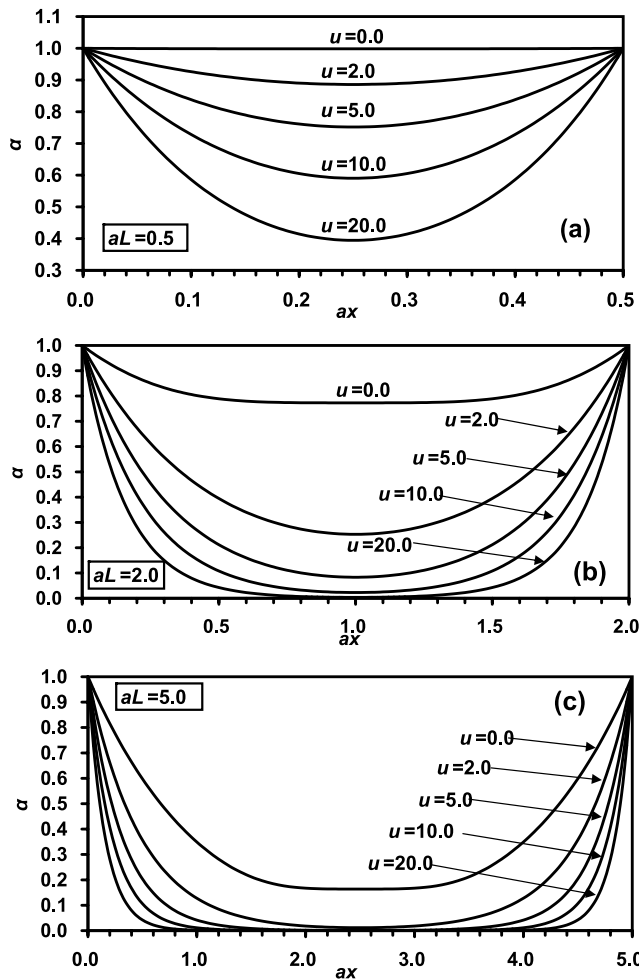


**Figure 2.** Changes of the head fluctuation amplitude at the middle line  $x = 0.5L$  with  $ax$  for different values of  $u$  when (a)  $aL = 0.5$ , (b)  $aL = 2.0$ , and (c)  $aL = 5.0$ .

the solution to the boundary value problem (6a), can be shown to be

$$X(x) = \frac{A_1 \sinh(L\lambda - \lambda x) + A_2 \exp(i\theta) \sinh(\lambda x)}{\sinh(L\lambda)}, 0 \leq x \leq L. \tag{7}$$

Then, the solution of the boundary value problem (1), (2) and (3) is

$$h(x, t) = \text{Re}\{X(x) \exp(-i\omega t)\} = A_1 \alpha \cos(\omega t - \varphi), 0 \leq x \leq L. \tag{8}$$

where  $\alpha$  and  $\varphi$  are the amplitude [L] and the phase shift (radian) of the tidal head fluctuation defined as

$$\alpha = \frac{1}{A_1} \left| \frac{A_1 \sinh(L\lambda - \lambda x) + A_2 \exp(i\theta) \sinh(\lambda x)}{\sinh(L\lambda)} \right| \tag{9}$$

$$\varphi = -\arg \frac{A_1 \sinh(L\lambda - \lambda x) + A_2 \exp(i\theta) \sinh(\lambda x)}{\sinh(L\lambda)}. \tag{10}$$

For an impermeable roof ( $K' = 0$ ) equation (8) reduces to that of *Rotzoll et al.* [2008], whence, taking the limit  $L \rightarrow \infty$ , our solution (8) is simplified into that of *Jacob* [1950]. Setting  $A_1 = A_2 = 1$  and  $\theta = 0$ , equation (8) can be simplified into the case considered by *Townley* [1995] in his ‘‘Example 1.’’

### 3. Effects of Aquifer’s Length and the Aquifer Roof’s Leakage

[9] For convenience, we only consider the special case when the tides at both sides of the island are the same (i.e.,  $A_1 = A_2 = A$ , and  $\theta = 0$ ).

[10] Figure 2 shows how the head fluctuation amplitude changes with  $ax$  for different values of  $u$  and dimensionless aquifer length  $aL$ . For any fixed point  $ax$  in the aquifer, the amplitude coefficient  $\alpha$  is always a decreasing function of  $u$ , indicating the damping effect of  $u$  on the groundwater head fluctuation.

[11] In Figure 2a ( $aL = 0.5$ ), because of the small dimensionless length of the aquifer, the amplitude coefficient  $\alpha$  is nearly constant when the leakage  $u = 0$ . For larger values of  $u$ , because the water levels experience fluctuations from both boundaries, the amplitude coefficient  $\alpha$  decreases from both sides to the minimum at the middle of the aquifer. Because of the short dimensionless aquifer length, the minimum of  $\alpha$  at the middle of the aquifer is greater than 0.4 for all the cases. In Figure 2b ( $aL = 2.0$ ), the aquifer’s length is larger, and the minimum of the amplitude coefficient  $\alpha$  at the middle of the aquifer is close to zero when  $u \geq 10$ . In Figure 2c ( $aL = 5.0$ ), the aquifer’s dimensionless

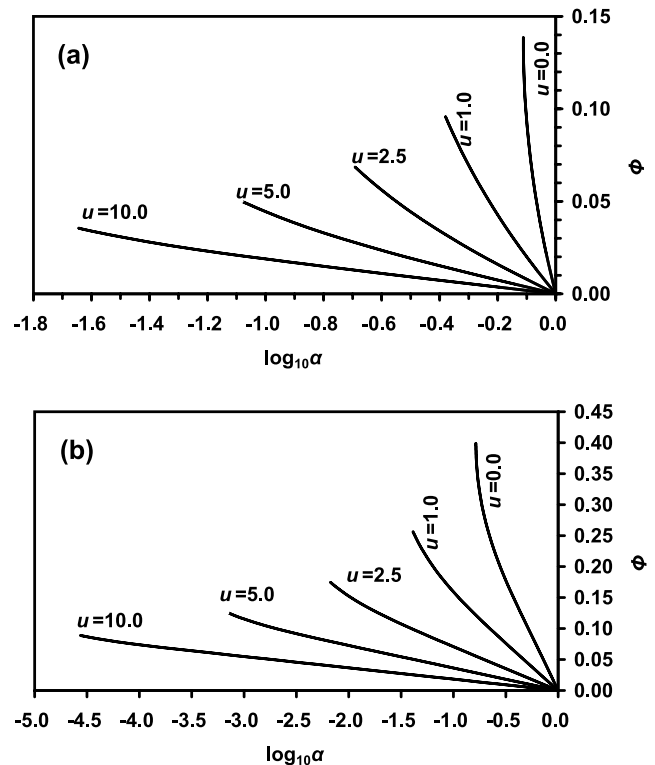


**Figure 3.** Changes of phase lag with log attenuation ( $\log_{10} \alpha$ ) for different values of leakage when (a)  $aL = 2.0$  and (b)  $aL = 5.0$ .

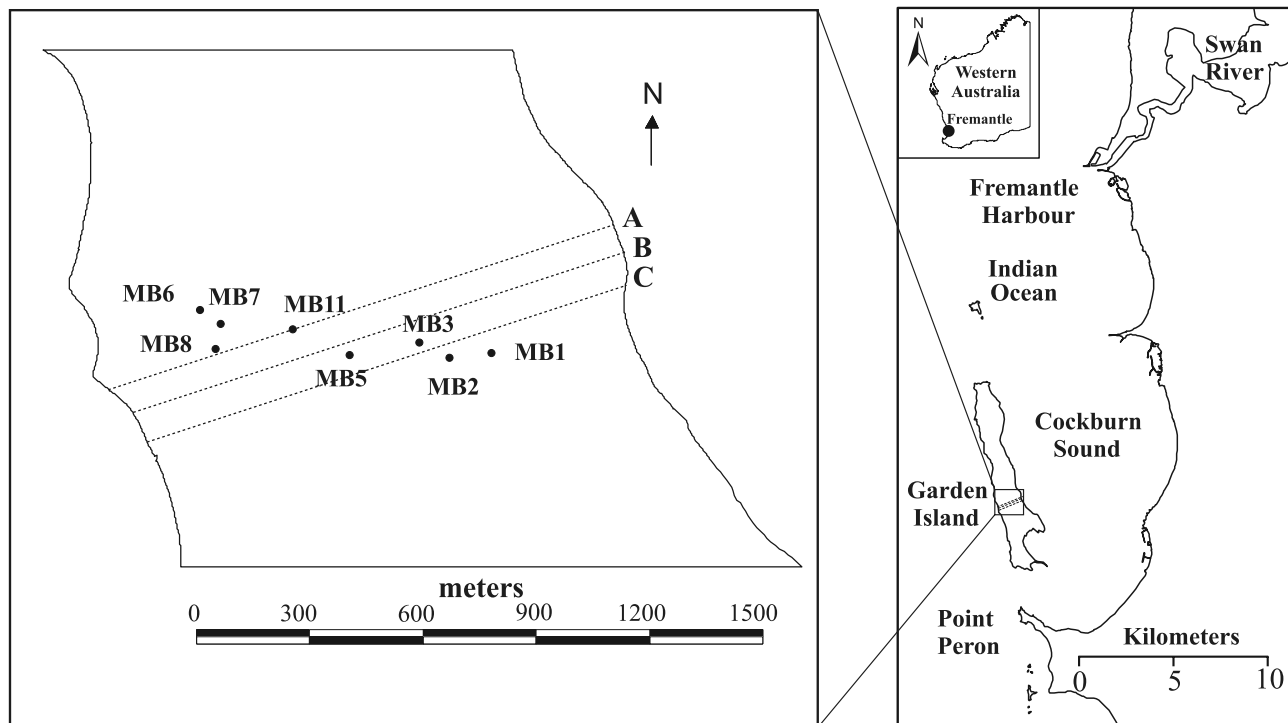


**Figure 4.** Locations of Garden Island ( $32^{\circ}12'S$ ,  $115^{\circ}40'E$ ), the eight monitoring wells and the three transects A, B, and C in Garden Island [after *Trefry and Bekele*, 2004].

length is the largest, and the mixed response from the two sides vanishes at the middle of the aquifer when  $u \geq 2.0$ .

[12] Figure 3 shows how the phase lag  $\Phi$  changes with log attenuation ( $\log \alpha$ ) for different values of  $u$  and  $aL$ . The phase lag  $\Phi$  is defined as  $\Phi = \varphi/(2\pi)$  where  $\varphi$  is the phase shift given by (10). At the coastline, the groundwater head fluctuates exactly as the tides do, so both the log attenuation and phase lag vanish for any values of  $u$  and  $aL$ . Therefore the origin ( $\log \alpha = 0$ ,  $\Phi = 0$ ) is the common point of all the curves. Since the amplitude coefficient  $\alpha$  decreases from both sides to the minimum at the middle of the aquifer and the phase lag  $\Phi$  increases from both sides to the maximum at the middle of the aquifer, each curve starts from the origin and extends in the up left direction to the end, which corresponds to the log attenuation and phase lag at the middle of the aquifer. As the log attenuation decreases, the phase lag increases approximately linearly for all the cases in Figures 3a and 3b. The greater  $u$ , the smaller the rate of increase. This indicates that the vertical leakage through the semipermeable layer, which is characterized by  $u$ , has significant effect in reducing the phase lag (or equivalently to shorten the time lag) in the whole aquifer. For example, in Figure 3b, for the fixed value of  $\log_{10} \alpha = -0.6$ , when  $u$  increases from 0.0 to 1.0, the phase lag decreases from 0.22 to 0.09. The greater  $u$ , the more significant the shortening effect on the phase lag in the aquifer.

[13] Figure 3 clearly shows that the vertical leakage term is able to induce the propagation bias (small time lag and significant amplitude attenuation). In reality, besides the vertical leakage, other factors may also lead to small time lag and significant amplitude attenuation. For example, *Li et al.* [2007] and *Liu et al.* [2008] showed that if the submarine outlet of a coastal confined aquifer is capped with less permeable sediment, negative phase shift may occur in

hydraulic head in offshore aquifers, which may result in very small time lag in inland aquifers near the coastline. Identification of the reason for the propagation bias needs the information of the aquifer structure and seaward boundary condition.

## 4. Application

[14] *Trefry and Bekele* [2004] observed and analyzed tide-induced groundwater level fluctuation data collected from Garden Island, Australia in 57 days. Various existing analytical solutions of ocean tidal propagation in bounded one-dimensional aquifers were tested but they could not predict the observed tidal propagation bias, i.e., the inconsistency between the observed strong amplitude attenuation and small time lag. In this section the solution (8) will be used to analyze the tidal effect at Garden Island. All the hydrogeologic data and information in this section are taken from *Trefry and Bekele* [2004] and references therein.

### 4.1. Hydrogeological Background and Conceptual Model

[15] Garden Island is located on the continental shelf of Western Australia. It is 10 km long from north to south and 2 km wide at its widest point (Figure 4). The formations of Garden Island vary in the sequence from top to bottom. Surface sediments are formed from leached and weakly lithified, fine-to-medium-grained sand dunes of the Safety Bay Sand formation. Next in the sequence is the Tamala limestone formation, a coarse-to-medium-grained calcarenite with variable amounts of sand [*Playford et al.*, 1976]. Next is a thick layer of Mesozoic shales and siltstones. This layer is assumed to be horizontal with the limestone interface located several tens of meters below sea level [*Davidson*, 1995, pp. 28 and 198] and forms a uniform

**Table 1.** Data of Aquifer Transects, Tidal Attenuations  $\alpha$  and Phase Lags  $\Phi$  Calculated From the 57-Day Time Series<sup>a</sup>

| Well       | $x_i^b$ (m) |            |            | K1 Mode  |        | O1 Mode  |        |
|------------|-------------|------------|------------|----------|--------|----------|--------|
|            | Transect A  | Transect B | Transect C | $\alpha$ | $\Phi$ | $\alpha$ | $\Phi$ |
|            | West coast  | 0          | 0          | 0        | 1      | 0        | 1      |
| MB6        | 296         | 254        | 242        | 0.119    | 0.120  | 0.059    | 0.219  |
| MB8        | 299         | 256        | 245        | 0.108    | 0.283  | 0.113    | 0.272  |
| MB7        | 336         | 293        | 282        | 0.069    | 0.199  | 0.074    | 0.186  |
| MB11       | 513         | 471        | 460        | 0.014    | 0.325  | 0.008    | 0.297  |
| MB5        | 633         | 590        | 579        | 0.007    | 0.407  | 0.003    | 0.375  |
| MB3        | 820         | 778        | 767        | 0.024    | 0.238  | 0.025    | 0.232  |
| MB2        | 881         | 839        | 827        | 0.040    | 0.229  | 0.040    | 0.192  |
| MB1        | 993         | 951        | 940        | 0.094    | 0.135  | 0.103    | 0.126  |
| East coast | 1420        | 1380       | 1340       | 1        | 0      | 1        | 0      |

<sup>a</sup>After *Trefry and Bekele* [2004, Tables 1 and 2].

<sup>b</sup>The well location  $x_i$  is the distance projected on the transects A, B and C and is listed in order from west to east along the transects.

impermeable bottom to the aquifer system throughout the study area. Both the geologic cross section information of Garden Island [*Trefry and Bekele*, 2004, Figures 2, 3, and 4] and the numerical results conducted by *Trefry and Bekele* [2004] supported a conceptual stratigraphic model of a highly permeable stratum underlying a semipermeable, superficial sand layer. The analyses of *Trefry and Bekele* [2004] also excluded the effect of the sloping beach on the tide-induced groundwater head fluctuation.

[16] The interface between the top semipermeable sand stratum and lower permeable limestone stratum is complex. Although a conceptual model of the interface dipping to the west was supposed by *Trefry and Bekele* [2004], it was not supported by the on-transect well logs, which show Tamala limestone at higher elevations toward the western end of the transect and an absence of limestone at depth toward the eastern side. Here, we simply regard the medium-grained sand and the limestone as a whole aquifer which is assumed to have a horizontal interface with its overlying fine-grained sand layer. As a result, the transect of Garden Island is simplified into a conceptual model as shown in Figure 1 and the analytical solution (8) can be used to describe the tidal groundwater flow.

#### 4.2. Aquifer Parameter Estimation

[17] *Trefry and Bekele* [2004] conducted Fourier spectra analyses to the 57-day head and tidal level time series and found that both the local tides and the head time series are diurnal with dominant O1 and K1 modes. Table 1 gives their estimations of the attenuation and phase lag of the O1

and K1 modes from the time series in the 8 monitoring wells. In order to use one-dimensional analytical solutions to fit the attenuations and phase lags in Table 1, *Trefry and Bekele* [2004] chose three transects (transects A, B and C; see Figure 4) through the island approximately from west to east in the vicinity of the group of the 8 monitoring wells. The well coordinates ( $x_i$ , projected perpendicularly onto each transect) are also listed in Table 1.

[18] In order to use our new solution (8) to fit the attenuations and phase lags in Table 1, following *Trefry and Bekele* [2004], at each monitoring well  $x_i$  we define the phase lag  $\Phi$  predicted by equation (10) as

$$\Phi(x_i; a, u) = \begin{cases} 1 + \frac{\varphi(x_i; a, u)}{2\pi}, & -\pi \leq \varphi < 0 \\ \frac{\varphi(x_i; a, u)}{2\pi}, & 0 \leq \varphi < \pi. \end{cases} \quad (11)$$

The attenuation coefficient  $\alpha(x_i, a, u)$  at each monitoring well  $x_i$  is given by equation (9). Then we minimized the following least squares objective function with respect to the two unknown parameters  $a$  and  $u$ ,

$$O_{\alpha, \Phi}(a, u) = \sum_{i=1}^8 [\log \alpha_i - \alpha(x_i; a, u)]^2 + [\Phi_i - \Phi(x_i; a, u)]^2, \quad (12)$$

where  $\alpha_i$  and  $\Phi_i$  are the observed attenuation coefficient and phase lag at the  $i$ th monitoring well listed in Table 1, respectively.

[19] The objective function (12) is the same as that used by *Trefry and Bekele* [2004] (equation (19) in their paper). A FORTAN code was developed to solve numerically the least squares problem (12) using quasi-Newton iteration method. For all the different initial parameter guess values, the converged parameter values of  $a$  and  $u$  are the same if the global minimum is reached. The objective function (12) was minimized both for O1 and K1 modes at the three transects A, B and C. Thus 6 estimated values were obtained both for  $a$  and  $u$ . The estimated value of  $a$  was then used to calculate the diffusivity  $D = T/S$  using the equation (4) and the frequencies of O1 and K1 ( $\omega = 0.930 \text{ d}^{-1}$  for O1 mode and  $1.003 \text{ d}^{-1}$  for K1 mode), and the estimated value of  $u$  was used to calculate the ratio of the leakance to the aquifer storativity ( $K'/(M_1 S)$ ) using the equation (5) and the frequencies of O1 and K1. Finally the ratio of the diffusivity to the quantity  $K'/(M_1 S)$  was calculated to obtain the estimation of  $TM_1/K'$ . The results are listed in Table 2. The

**Table 2.** Aquifer Diffusivities  $D$  and Dimensionless Leakage  $u$  Estimated From Minimizing the Objective Function (12) for the Two Tidal Modes K1 and O1<sup>a</sup>

| Transect | O1 Mode, $\omega = 0.930 \text{ d}^{-1}$  |       |                            |             | K1 Mode, $\omega = 1.003 \text{ d}^{-1}$  |       |                            |             |
|----------|-------------------------------------------|-------|----------------------------|-------------|-------------------------------------------|-------|----------------------------|-------------|
|          | $D = T/S$ ( $\text{m}^2 \text{ d}^{-1}$ ) | $u$   | $TM_1/K'$ ( $\text{m}^2$ ) | SS          | $D = T/S$ ( $\text{m}^2 \text{ d}^{-1}$ ) | $u$   | $TM_1/K'$ ( $\text{m}^2$ ) | SS          |
| A        | 20149 (61500)                             | 1.082 | 20023                      | 0.98 (1.67) | 22304 (72100)                             | 0.923 | 24092                      | 0.41 (1.03) |
| B        | 18927 (55200)                             | 1.092 | 18637                      | 1.33 (1.94) | 20870 (67100)                             | 0.935 | 22254                      | 0.64 (1.26) |
| C        | 17363 (50800)                             | 1.093 | 17081                      | 1.21 (1.83) | 19116 (61800)                             | 0.93  | 20493                      | 0.56 (1.19) |
| Average  | 18813 (55800)                             | 1.089 | 18581                      |             | 20763 (67000)                             | 0.929 | 22280                      |             |

<sup>a</sup>Values are presented for the three transects as shown in Figure 5 and Table 1. Averaged values on the three transects are given in the last row. The notation SS denotes the objective function value (sum of squares) at the regression optimum. The values of  $D$  and SS calculated by *Trefry and Bekele* [2004, Table 3] using the one-dimensional homogeneous aquifer model are listed in parentheses for comparison.

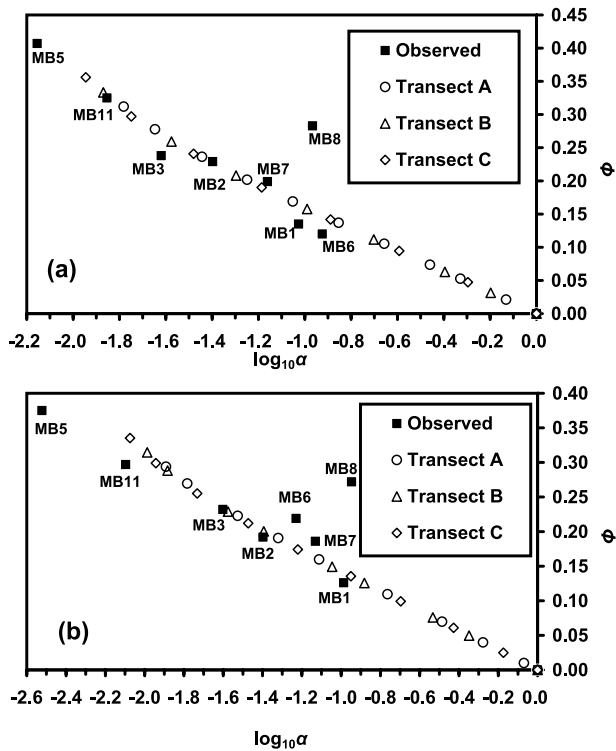


**Figure 5.** Regression results of typical (a) K1 and (b) O1 modes for the three transects A, B, and C.

estimations of  $TM_1/K'$  based on O1 and K1 modes have an average of  $20430 \text{ m}^2$ . If one knows the value  $M_1$  and the aquifer thickness, one can obtain an estimation of the permeability ratio of the aquifer to the semipermeable sand layer. For example, if  $M_1 = 10 \text{ m}$ , the aquifer thickness is  $30 \text{ m}$ , then the averaged value  $20430 \text{ m}^2$  of  $TM_1/K'$  yields a value of about 68 for the permeability ratio of the aquifer to the semipermeable layer.

[20] The minimum values (SS) of the objective function (12) are also listed in Table 2. Compared with the SS values in the brackets based on the one-dimensional homogeneous single aquifer models, the solution (8) gave considerably improved least squares fittings. Figure 5 shows the best fit curves for the three transects A, B and C in  $\log$  (attenuation) lag space; the eight data points ( $\log_{10} \alpha_i, \Phi_i$ ) in Table 1 are also shown in solid squares for comparison. The three curves corresponding to the three transects A, B and C nearly coincide with each other both for K1 and O1 modes. The fitting curves for K1 and O1 modes are satisfactorily close to the measurement data points except the well MB8, where exceptionally large phase shifts were observed both for K1 and O1 modes. This exception was probably caused by local heterogeneity near MB8 (e.g., smaller  $u$  value near MB8 than elsewhere), which is obviously beyond the scope of this analytical study.

[21] *Trefry and Bekele* [2004, Figures 6c and 6f] compared the 8 data points with their best fit curves obtained from the one-dimensional homogeneous and composite aquifer models, where the best fit curves are always above the data points, a phenomenon called “propagation bias” by *Trefry and Bekele* [2004]. On the basis of their numerical

experiments, *Trefry and Bekele* [2004] suggested that the most probable cause of the propagation bias was the horizontal layering in aquifer properties, and that the analysis of measured propagation bias has the potential to yield extra information on aquifer properties in the vertical direction. Our results here confirmed their suggestions.

## 5. Conclusions

[22] This paper presents an analytical solution of groundwater head response to dual-tide fluctuation in a leaky aquifer system representing the transect of an island. The system comprises a confined aquifer and a semipermeable layer (the confined aquifer’s roof). Both the confined aquifer and its roof terminate at the coastlines. Previous studies of tidal groundwater flow considered either the tidal forcing on one boundary of the aquifer or neglected the leakage through the aquifer’s roof. This paper incorporates the effects of both the dual tide and the leakage through the semipermeable roof. Solution analysis indicates that the tidal wave interference from the two sides of the island transect decreases to zero as the horizontal length of the aquifer increases to infinity. The leakage of the overlying confining layer enhances the landward attenuation of the tidal head fluctuation and shortens the time lag between the head and tide fluctuations. Our new solution was used to analyze the leakage effect of the overlying semipermeable layer in tide-induced groundwater head fluctuations at Garden Island. The solution agreed well with the observations in eight piezometers in Garden Island, Australia.

[23] **Acknowledgments.** This research was supported by the National Natural Science Foundation of China (40672167) and was also supported by the 111 Project (B08030). We are very grateful for the helpful review comments from three anonymous reviewers.

## References

- Davidson, W. A. (1995), Hydrogeology and groundwater resources of the Perth region, Western Australia, *Bull.*, 142, pp. 49–60, West. Aust. Geol. Surv., Perth, West. Aust., Australia.
- Droge, C., M. Razark, and P. Krivic (1984), Survey of a coastal karstic aquifer by analysis of the effect of karst of Slovenia, Yugoslavia, *Environ. Geol. Water Sci.*, 6, 103–109, doi:10.1007/BF02509916.
- Hantush, M. S. (1960), Modification of the theory of leaky aquifers, *J. Geophys. Res.*, 65, 3713–3716, doi:10.1029/JZ065i011p03713.
- Jacob, C. E. (1950), Flow of groundwater, in *Engineering Hydraulics*, edited by H. Rouse, pp. 321–386, John Wiley, Hoboken, N. J.
- Jeng, D.-S., L. Li, and D. A. Barry (2002), Analytical solution for tidal propagation in a coupled semi-confined/phreatic coastal aquifer, *Adv. Water Resour.*, 25, 577–584, doi:10.1016/S0309-1708(02)00016-7.
- Jiao, J. J., and Z. Tang (1999), An analytical solution of groundwater response to tidal fluctuation in a leaky confined aquifer, *Water Resour. Res.*, 35, 747–751, doi:10.1029/1998WR900075.
- Li, H., and J. J. Jiao (2001a), Tide-induced groundwater fluctuation in a coastal leaky confined aquifer system extending under the sea, *Water Resour. Res.*, 37, 1165–1171, doi:10.1029/2000WR900296.
- Li, H., and J. J. Jiao (2001b), Analytical studies of groundwater-head fluctuation in a coastal confined aquifer overlain by a leaky layer with storage, *Adv. Water Resour.*, 24, 565–573, doi:10.1016/S0309-1708(00)00074-9.
- Li, H., and J. J. Jiao (2002a), Analytical solutions of tidal groundwater flow in coastal two-aquifer system, *Adv. Water Resour.*, 25, 417–426, doi:10.1016/S0309-1708(02)00004-0.
- Li, H., and J. J. Jiao (2002b), Tidal groundwater level fluctuations in L-shaped leaky coastal aquifer system, *J. Hydrol.*, 268, 234–243, doi:10.1016/S0022-1694(02)00177-4.
- Li, H., and J. J. Jiao (2003), Tide-induced seawater-groundwater circulation in a multi-layered coastal leaky aquifer system, *J. Hydrol.*, 274, 211–224, doi:10.1016/S0022-1694(02)00413-4.

- Li, H., and Q. C. Yang (2000), A least-squares penalty method algorithm for the inverse problem of steady state aquifer models, *Adv. Water Resour.*, 23, 867–880, doi:10.1016/S0309-1708(00)00018-X.
- Li, H., J. J. Jiao, M. Luk, and K. Cheung (2002), Tide-induced groundwater level fluctuation in coastal aquifers bounded by L-shaped coastlines, *Water Resour. Res.*, 38(3), 1024, doi:10.1029/2001WR000556.
- Li, H., G. Y. Li, J. M. Cheng, and M. C. Boufadel (2007), Tide-induced head fluctuations in a confined aquifer with sediment covering its outlet at the sea floor, *Water Resour. Res.*, 43, W03404, doi:10.1029/2005WR004724.
- Li, L., D. A. Barry, and D.-S. Jeng (2001), Tidal fluctuations in a leaky confined aquifer: Dynamic effects of an overlying phreatic aquifer, *Water Resour. Res.*, 37, 1095–1098, doi:10.1029/2000WR900402.
- Liu, S., H. L. Li, M. C. Boufadel, and G. H. Li (2008), Numerical simulation of the effect of the sloping submarine outlet-capping on tidal groundwater head fluctuation in confined coastal aquifers, *J. Hydrol.*, 361, 339–348.
- Neuman, S. P., and P. A. Witherspoon (1969), Theory of flow in a confined two aquifer system, *Water Resour. Res.*, 5, 803–816, doi:10.1029/WR005i004p00803.
- Playford, P. E., A. E. Cockbain, and G. H. Low (1976), Geology of the Perth Basin, Western Australia, *Bull. 124*, 311 pp., West. Aust. Geol. Surv., Perth, West. Aust., Australia.
- Rotzoll, K., A. I. El-Kadi, and S. B. Gingerich (2008), Analysis of an unconfined aquifer subject to asynchronous dual-tide propagation, *Ground Water*, 46, 239–250, doi:10.1111/j.1745-6584.2007.00412.x.
- Sun, H. (1997), A two-dimensional analytical solution of groundwater response to tidal loading in an estuary, *Water Resour. Res.*, 33, 1429–1435, doi:10.1029/97WR00482.
- Townley, L. R. (1995), The response of aquifers to periodic forcing, *Adv. Water Resour.*, 18, 125–146, doi:10.1016/0309-1708(95)00008-7.
- Trefry, M. G. (1999), Periodic forcing in composite aquifers, *Adv. Water Resour.*, 22, 645–656, doi:10.1016/S0309-1708(98)00037-2.
- Trefry, M. G., and E. Bekele (2004), Structural characterization of an island aquifer via tidal methods, *Water Resour. Res.*, 40, W01505, doi:10.1029/2003WR002003.

---

M. C. Boufadel, Department of Civil and Environmental Engineering, Temple University, 1947 North 12th Street, Philadelphia, PA 19122, USA. (boufadel@temple.edu)

S. Chen, H. Li, and P. Sun, School of Environmental Studies, China University of Geosciences, Wuhan 430074, China. (aliphonse@gmail.com; hailong@graduate.hku.hk; sunpingping203@gmail.com)

X. Geng, Department of Mathematics, Anshan Normal University, Anshan 114005, China. (gengxiaolong@gmail.com)